HHS Public Access

Author manuscript

Tuberculosis (Edinb). Author manuscript; available in PMC 2020 May 01.

Published in final edited form as:

Tuberculosis (Edinb). 2019 May ; 116 Suppl: S118–S122. doi:10.1016/j.tube.2019.04.019.

Mycobacterial Trehalose 6,6'-dimycolate Induced Vascular Occlusion is Accompanied by Subendothelial Inflammation

Shen-An Hwang[1], **Caitlan D. Byerly**[1], and **Jeffrey K. Actor**[1]

[1]Department of Pathology and Laboratory Medicine, UTHealth McGovern Medical School, Houston, TX, USA.

Abstract

Mycobacterium tuberculosis (MTB) is a pathogen that infects and kills millions yearly. The mycobacterium's cell wall glycolipid trehalose 6,6'-dimycolate (TDM) has been used historically to model MTB induced inflammation and granuloma formation. Alterations to the model can significantly influence the induced pathology. One such method incorporates intraperitoneal pre-exposure, after which the intravenous injection of TDM generates pathological damage effectively mimicking the hypercoagulation, thrombus formation, and tissue remodeling apparent in lungs of infected individuals. The purpose of these experiments is to examine the histological inflammation involved in the TDM mouse model that induces development of the hemorrhagic response. TDM induced lungs of C57BL/6 mice to undergo granulomatous inflammation. Further histological examination of the peak response demonstrated tissue remodeling consistent with hypercoagulation. The observed vascular occlusion indicates that obstruction likely occurs due to subendothelial localized activity leading to restriction of blood vessel lumens. Trichrome staining revealed that associated damage in the hypercoagulation model is consistent with intra endothelial cell accumulation of innate cells, bordered by collagen deposition in the underlying parenchyma. Overall, the hypercoagulation model represents a comparative pathological instrument for understanding mechanisms underlying development of hemorrhage and vascular occlusion seen during MTB infection.

Keywords

Tuberculosis; trehalose 6,6'-dimycolate; Granuloma; Immunopathology

1. Introduction

It is well accepted that inflammatory and hemostatic pathways are engaged during acute infections. Specific coagulation occurs at sites of bacterial replication, presumably as an

Corresponding Author: Jeffrey K. Actor, Ph.D., Professor, Department of Pathology and Laboratory Medicine, MSB 2.214, UTHealth McGovern Medical School, 6431 Fannin, Houston, TX 77030, Tel: (713) 500-5344; Fax: (713)-500-0730, Jeffrey.K.Actor@uth.tmc.edu.

evolved mechanism to limit organism dissemination. The two related pathways converge; factors released during the kinin and clotting cascades eventually trigger complement activation which directly impacts the innate inflammatory response. Indeed, many organisms have evolved to secrete factors that suppress fibrinolytic channels, to overcome this “innate” power of the coagulation system to halt spread of disease. For example, both *Yersinia pestis* and Group A streptococci demonstrate mechanisms with the end result of fibrin degradation to limit the effects of host coagulation to contain organisms[1, 2]. Of interest, systemic responses do not always correlate with tissue specific events; in many instances increased coagulation factors appear in serum concurrent with decreased presence of anticoagulant factors in lungs of individuals with pulmonary infections[3].

It is not uncommon to expect hemostatic changes in patients with active tuberculosis (TB), especially when considering the extent of pulmonary tissue damage at later stages of disease[4]. Indeed, individuals with severe active pulmonary *Mycobacterium tuberculosis* infection demonstrate upregulated anti-coagulant activity, evident as elevated plasma fibrinogen with depressed antithrombin activity[5, 6]. General suppression of fibrinolytic cascading events can also be found in individuals with primary infection. This is expressed as increased circulating fibrinogen within serum, thus linking clinical presentation and reported incidence of thrombosis and petechial hemorrhage in those patients as well. Specifically, it was reported that tissue-type plasminogen activator (tPA) was elevated in the plasma of primary TB individuals[7], coinciding with elevated TB-related biomarkers in serum. However, in the same study, bronchoalveolar lavage fluid (BAL) collected from patients with suspected pulmonary TB did not demonstrate clear evidence for coagulation activation specifically at the site of inflammatory disease.

Mouse models to examine the observed hypercoagulation phenomena provide the opportunity to synchronize the inflammatory events and study pathological change induced during initial granulomata formation. In the 1950’s, a hemorrhagic model of lung pathology related to mycobacterial infection was investigated, induced by repeated intraperitoneal administration of crude cord factor[8]. 30 years later, Seggev, Goren and colleagues furthered these experiments to investigate the ensuing pneumonitis[9, 10]. Their experiments detailed an interstitial and hemorrhagic pneumonitis produced following a single injection of TDM (in light mineral oil) in C57BL/6 mice; with further note of the transient nature of the lesion with peak response at 7–9 days post injection. In 1994, Perez, et al., returned to this subject to examine extravascular coagulation and fibrinolysis induced in a more refined model of TB granulomatous response, using the purified cord factor component trehalose-6,6’-dimycolate (TDM)[11]. They found that procoagulant activity increased during productive granuloma events. However, in hindsight, the model had been adapted to intravenous administration of TDM to promote a synchronized transient granulomatous response. While this allowed assessment of factors involved in development of the granuloma[12–14], the model no longer accurately represented events during primary tuberculosis infection in which pulmonary hemorrhage occurs.

Recently, Donnachie, et al., was successful at repeating the pathology induced by the earlier methodologies of Block and Noll, using purified TDM[15]. They comparatively assessed the different formats of TDM administration, and identified unique cytokine and histological

profiles present in the original cord factor model that were not present in the model adapted for direct granulomatous response. Their “hypercoagulation” model more accurately represented vascular occlusion and blood thickening seen in human disease. The studies here build on their basic findings, and further examine the nature of the histopathology related to the induced vascular occlusion caused by administration of TDM.

2. Materials and Method

Mice.

Female C57BL/6 mice (Jackson Laboratories) of approximate 20g initial body weight were utilized for the study. Mice were six to eight weeks of age at initiation of experiments. All animal work was performed under the approval of the University of Texas Health Science Center (UTHSC) animal welfare committee, documents HSC-AWC-13–123 and HSC-AWC-17–0089).

TDM Induced Lung Pathology.

Mtb derived TDM (cord factor) (Enzo Life Sciences, Farmingdale, NY) was solubilized in hexane:ethanol, at a ratio of 9:1), and evaporated under stream of air. TDM (50 μg/mouse) in oil was prepared by homogenization in Drakeol (100 μL/mouse) (Penreco, Indianapolis, IN) in a glass tube and Teflon pestle for 1 min. The TDM in oil formulation was intraperitoneally (IP) delivered. The TDM oil/water emulsion was prepared as previously described[14]. Briefly, evaporated TDM (10 or 25 μg/mouse) was homogenized in Drakeol (2 μL/mouse), 48 μL/mouse of 1x DPBS (Dulbeccos’ Phosphate Buffered Solution, Cellgro) with 0.2% Tween 80 (Mallinckrodt, Hazelwood, MO) was added and homongenized. The TDM oil/water emulsion were intravenously (IV) administered. Controls included formulations with no TDM in oil. Emulsion only controls did not exhibit inflammation at the times described, as previously reported and detailed[12, 16].

C57BL/6 mice groups were treated as follows: “Control” mice were naïve, without injections. “Oil – IP only” received oil only injected IP without TDM. “Oil/water–IV” received an IV injection of oil/water emulsion without TDM. “TDM–IP” – received IP injections of 10μg TDM in Drakeol (100μL/mouse). “TDM–IV Acute” received IV injections of 10μg or 25μg TDM in Drakeol (100μL/mouse). “TDM–IPIV Hypercoagulation” – received 10μg TDM in Drakeol (100μL/mouse) injected IP followed by an IV injection after 7 days of 10 μg/mouse TDM in Drakeol (100μL/mouse). All mice were sacrificed at day 7 post final TDM or control formulation injections.

Histological Assessment.

Upon sacrifice, lungs were perfused with 1mM EDTA in DPBS. Lungs were weighed, and sectioned to evaluate pathology and histological outcomes. Tissues for histology were fixed in 10% buffered formalin (Fisher Scientific, Pittsburg, PA). Processing of the specimens was performed by the Histology Laboratory at the McGovern Medical School (Houston, TX). Tissues were embedded in paraffin blocks and 5 μm thick sections were prepared and stained with hematoxylin (Surgipath, Richmond, IL) and eosin (Richard-Allen Scientific, Kalamazoo, MI) (H&E).

Lung weight index (LWI).

Lung weight index (LWI) was calculated as a rough measure of lung inflammation intensity[12, 17] using the following equation, adapted for detection of gross tissue inflammation due to induced BCG infection in susceptible and resistant[17] or lymphocyte deficient mice[18]:

$$\mathbf{LWI} = \frac{\sqrt{\frac{\mathbf{Lung\ weight\ (g)} \times \mathbf{1000}}{\mathbf{Mouse\ weight\ (g)\ /\ 10}}}}{\mathbf{10}}$$

Immunohistochemical analysis.

The large right lobe of the lung is collected and fixed in 10% buffered formalin. For analysis, fixed lung was stained with hematoxylin and eosin (H & E) or Masson's Trichrome as per standard procedures. Immunohistochemical examination of Vascular Endothelial Cadherin, CD144, diluted at 1:200, was performed according to manufacturer's instructions, and visualized using standard HRP techniques using the "Vectastain ABC method" (Vector Laboratories, Burlingame, CA). Stained slides were viewed by a trained pathologist, with descriptive results obtained in an experimentally blinded manner.

Statistical Analysis.

Data obtained was compared across groups, and against naive mice or mice challenged with formulation vehicle alone, then analyzed by an unpaired *t*-test or two-way ANOVA; differences between means were significant at a level of $p \leq 0.05$. Data are presented as a compilation of all experimental repeats (2 or 3). Each experiment has N = 4–6 mice.

3. Results

Comparison of TDM Induced Pathology: Hypercoagulation vs Acute Models.

Inflammation was induced in lung tissue of C57BL/6 mice injected with MTB derived TDM, comparing several different methodologies. These included controls of TDM in oil given intraperitoneally (TDM-IP); the acute TDM model with TDM in oil/water given intravenously (TDM-IV Acute); and TDM given IP followed 7 days later with TDM given IV (TDM-IPIV Hypercoagulation). Controls included naïve mice, and mice given light mineral oil (no TDM) only IP at volumes equivalent to experimental groups.

General lung inflammation was assessed as lung weight index (LWI) at 7 days post IV TDM challenge, reflecting peak granulomatous response to TDM[12] [Figure 1]. As previously reported, TDM-IV Acute treatment increased LWI significantly, at both low (10 μg/mouse)[12] and mid-range (25 μg/mouse)[19] doses, with increased LWI presenting at the higher level. C57BL/6 mice given administered light mineral oil alone (no TDM) did not exhibit changes to LWI (not shown).

To replicate the hypercoagulation model, TDM was first administered IP at 10 μg/mouse in Drakeol, followed by IV administration at 10 μg/mouse TDM in oil/water emulsion[15]. Overall, the LWI was significantly elevated at day 7 post TDM administration, albeit with

higher variability in individual mice, in the TDP-IPIV Hypercoagulation model [Figure 1]. Mice given IP injections of TDM at 10 or 50 μg/mouse did not exhibit any significant change in LWI.

Histological Comparison of TDM Induced Pathologies.

Both the naïve and IP vehicle (no TDM) injected mice demonstrated no noticeable changes to lung architecture. These groups had normal pulmonary parenchyma with no noticeable changes in appearance due to cellular infiltrates, with only occasional very small clusters of leukocytes. These controls did not exhibit thickening of alveolar walls (not shown). As expected, mice administered TDM-IV at the lower dose (μg/mouse) demonstrated focal accumulation of macrophages after 7 days, but no apparent accumulation of lymphocytes (Figure 2). The mice receiving the higher dose of TDM (25 μg/mouse) demonstrated an increase in granuloma size and number compared to the lower dose group. The pathological reactivity also intensified, with reduction of open alveolar spaces, and widespread inflammation. In addition, lungs demonstrated small, focal hemorrhagic petechiae, albeit as a relatively minor component of the inflammatory response. Lymphocytic infiltration was apparent, predominantly occurring around regions where granulomas coincided with vasculature. In contrast, the hypercoagulation group experienced a markedly different pathological response. The inflammatory response was aggressive, with less focal reactivity. Both monocyte macrophages and lymphocytic infiltration was present, along with thickening of alveolar walls. Severe hemorrhage was present throughout the parenchyma, with obvious occlusion of blood vessels. Slight edema was present, although it was not a major component of the response.

Higher magnification to directly compare responses revealed that administration of TDM (25 μg/mouse) revealed lymphocytic cuffing around vascular beds, slight thickening of vascular walls, and occasional accumulation of cells and tissue debris within the vascular regions (Figure 3). Activated macrophages with intracellular vesicles were predominant in regions of reactivity. Although there was intense reactivity, there was minimal damage to the endothelial cell lining of vascular lumen and sublumen regions. In comparison, the hypercoagulation group experienced severe thickening of vascular walls, and extensive damage to the endothelial cell lining of vasculature. Vascular architecture was significantly modified around regions of granulomatous inflammation, with partial vascular occlusion due to the subendothelial modification.

Vascular Remodeling and Collagen Deposition during Hypercoagulation Events.

The vascular remodeling in the hypercoagulation model was further assessed using Trichrome stain. Extreme differences were identified between the two models. The acute IV administered TDM did not induce collagen deposition; only expected presence of collagen fibers were identified in regions localized to vascular beds. There was no significant alteration of collagen presence in epithelial regions that define alveolar spaces. In high contrast, the hypercoagulation model induced marked increase in collagen presence in areas surrounding regions of vascular occlusion. High powered magnification (Figure 4) identified collagen deposition, especially in regions of cellular activation present at subendothelial beds. Moreover, limited and smaller, but detectable, sites of collagen were identified near

regions of inflammation, appearing in alveolar linings where type II pneumocytes are expected to reside.

Vascular Occlusion Resulting from Subendothelial Region Parenchymal Inflammation.

Because both models resulted in inflammatory responses post intravenous injection, the tissues were further examined to determine if the vascular occlusion events were due to lodged complexes of TDM emulsion. Tissue was stained for the vascular endothelial cadherin marker present on endothelial cells lining vascular lumen (Figure 5). In both models, significant marker was present on cells lining blood vessels within the lung. Of major finding, the marker was not disrupted in the IV acute model, with clear appearance of intact endothelial cells lining blood vessel lumens. This was apparent regardless of inflammation surrounding the vascular region. In contrast, the hypercoagulation model exhibited disrupted endothelial contiguity, with incomplete regions of lumen lining. However, the subendothelial inflammation appeared separate from marker staining. This suggests that the disruption of subendothelial beds is the likely cause of vascular occlusion and hemorrhagicresponse, resulting from an intraperenchymal inflammatory event constricting lumen regions rather than caused by intraluminal deposition of IV administered TDM.

4. Discussion

The trehalose 6,6'-dimycolate of has been linked to both innate and adaptive inflammatory responses, much of which has been described in reports detailing focused animal models[20] or descriptive relevance to human disease[21]. The majority of studies focus on mechanisms underlying development of the induced inflammatory response; extensive efforts have been made to determine longitudinal events to establish the inflammatory granulomatous response[13] as well identify receptors that trigger distinct immune events[22]. However, it is also well established that the TDM molecule can trigger a different pathology, leading to pneumonitis with pronounced accompanying hemorrhagic response. This outcome of inflammation is not well studied, yet should be recognized as a distinct model that mimics hypercoagulation seen during tuberculosis infection.

Models of TDM (or cord factor) induced granulomatous response have previously demonstrated changes in coagulation components. Yet the exact nature of the coagulopathy was not extensively examined until recently[15]. Historic recognition of the coagulopathic involvement dates to 1955, when Bloch and Noll identified a component implicated in organism cording that resulted in hemorrhage upon injection into animals[8]. Their findings indicated that repeated injections of cord factor to C57 Black mice induced the "Schwartzman phenomenon" where toxic reactivity caused thrombosis. Kato and colleagues identified the chemical structure of cord factor as the mycolic acid trehalose 6,6'-dimycolate[23], which could be used to induce experimental "tubercules" nodules in lungs of mice after injection[24]. In the 1980's, Retzinger, et al., hinted at a relationship between the dissemination of TDM coated beads and possible coagulopathy[25], in part related to the conformational state of TDM[26]; TDM stabilized in oil emulsions showed hemorrhagic toxicity while saline formulations did not[27]. Perez, et al., speculated that hypercoagulation

was related to TDM induced fibrinolytic events, specifically within localized lung tissue responding to TDM[11]; they specifically detailed elevated procoagulant activity (PCA) in bronchoalveolar lavage following intravenous injection of TDM. Behling, et al, further demonstrated that both the granulomas and hemorrhagic toxic reactions were dependent on the dimycolate conformation; the two analogs, trehalose 6-monomycolate (TMM) and galactose-galactose 6, 6' dimycolate (GDM) were unable to induce pulmonary granulomas or hypercoagulant reactivity[27]. Sakamoto, et al, followed up on this finding nearly two decades later using intravenously administered TDM coated beads to reveal an involvement to pathways involved in the hydrolysis of fibrinogen to fibrin[28].

An interesting observation suggests that tissue factor expression by macrophages exposed to tuberculin is a key factor for the activation of blood coagulation pathways, and the resulting fibrin deposition. This was previously linked to development of hypersensitive delayed type responses[29]; it is quite possible that TDM is an active component to trigger this response, as demonstrated in the hypercoagulation model presented here. By this view, inflammation triggered by innate components controls hypercoagulation. However, it is more likely that endothelium also plays a central role in all both pathways involved in the pathogenesis, as they have been linked to the "hemostatic derangement" observed during pathogen induced severe inflammation[30]. Clearly, the pathogenesis of vascular disease has extensive cross-talk between both inflammatory and coagulatory pathways; inflammation leads to activation of coagulation, and coagulation affects inflammatory activity[31].

Remodeling of lung tissue with apparent collagen reorganization is readily apparent in clinical derived specimens from acute and post primary tuberculosis patients[32]. Collagen deposition has also been reported in animal models of infection[33]. The unique aspects apparent in the hypercoagulation model reported here also include changes in collagen localization and deposition, which was first reported by Donnachie, et al.[15]. Our study reconfirms this type of tissue remodeling in a non-infectious *M. tuberculosis* pulmonary pathological setting, and extends the observations to include subendothelial events as critical for vascular bed inflammation and disruption of blood vessel integrity. Overall, the hypercoagulation model may prove to be a useful tool to address pulmonary remodeling induced during mycobacterial infections. Furthermore, it may serve as an efficacious experimental tool to examine the cross-regulation of inflammatory factors and coagulation cascades that lead to pathological changes in models of pulmonary granulomatous diseases.

Acknowledgements.

We thank Dr. Robert L. Hunter, MD, PhD for insightful comments and review of pathological findings in this report.

This work was supported by NIH Grant 1R41-AI117990-02.

References

1. Sodeinde OA, Subrahmanyam YV, Stark K, Quan T, Bao Y, Goguen JD. A surface protease and the invasive character of plague. Science 1992;258:1004–1007. [PubMed: 1439793]

2. Sun H, Wang X, Degen JL, Ginsburg D. Reduced thrombin generation increases host susceptibility to group A streptococcal infection. Blood 2009;113:1358–1364. doi: 10.1182/blood-2008-07-170506 [PubMed: 19056689]

3. Esmon CT. Molecular circuits in thrombosis and inflammation. Thrombosis and haemostasis 2013;109:416–420. doi: 10.1160/TH12-08-0634 [PubMed: 23407677]

4. Robson SC, White NW, Aronson I, Woollgar R, Goodman H, Jacobs P. Acute-phase response and the hypercoagulable state in pulmonary tuberculosis. British journal of haematology 1996;93:943–949. [PubMed: 8703831]

5. Turken O, Kunter E, Sezer M, Solmazgul E, Cerrahoglu K, Bozkanat E, Ozturk A, Ilvan A. Hemostatic changes in active pulmonary tuberculosis. The international journal of tuberculosis and lung disease : the official journal of the International Union against Tuberculosis and Lung Disease 2002;6:927–932.

6. Sezer M, Ozturk A, Ilvan A, Ozkan M, Uskent N. The Hemostatic Changes in Active Pulmonary Tuberculosis. Turkish journal of haematology : official journal of Turkish Society of Haematology 2001;18:95–100. [PubMed: 27264063]

7. Kager LM, Blok DC, Lede IO, Rahman W, Afroz R, Bresser P, van der Zee JS, Ghose A, Visser CE, de Jong MD, Tanck MW, Zahed AS, Alam KM, Hassan M, Hossain A, Lutter R, Veer CV, Dondorp AM, Meijers JC, van der Poll T. Pulmonary tuberculosis induces a systemic hypercoagulable state. The Journal of infection 2015;70:324–334. doi: 10.1016/j.jinf.2014.10.006 [PubMed: 25455017]

8. Bloch H, Noll H. Studies on the virulence of Tubercle bacilli; the effect of cord factor on murine tuberculosis. British journal of experimental pathology 1955;36:8–17. [PubMed: 14351632]

9. Seggev J, Goren MB, Carr RI, Kirkpatrick CH. Interstitial and hemorrhagic pneumonitis induced by mycobacterial trehalose dimycolate. The American journal of pathology 1982;106:348–355. [PubMed: 6801989]

10. Seggev JS, Goren MB, Carr RI, Rubenstein E, Kirkpatrick CH. Pathogenesis of trehalose dimycolate-induced interstitial pneumonitis. IV. Evidence against roles for immunoglobulins and the complement system. Experimental lung research 1988;14:431–444. [PubMed: 3061788]

11. Perez RL, Roman J, Staton GW Jr., Hunter RL. Extravascular coagulation and fibrinolysis in murine lung inflammation induced by the mycobacterial cord factor trehalose-6,6'-dimycolate. American journal of respiratory and critical care medicine 1994;149:510–518. doi: 10.1164/ajrccm.149.2.8306054 [PubMed: 8306054]

12. Perez RL, Roman J, Roser S, Little C, Olsen M, Indrigo J, Hunter RL, Actor JK. Cytokine message and protein expression during lung granuloma formation and resolution induced by the mycobacterial cord factor trehalose-6,6'-dimycolate. Journal of interferon & cytokine research : the official journal of the International Society for Interferon and Cytokine Research 2000;20:795–804. doi: 10.1089/10799900050151067

13. Welsh KJ, Abbott AN, Hwang SA, Indrigo J, Armitige LY, Blackburn MR, Hunter RL Jr., Actor JK. A role for tumour necrosis factor-alpha, complement C5 and interleukin-6 in the initiation and development of the mycobacterial cord factor trehalose 6,6'-dimycolate induced granulomatous response. Microbiology 2008;154:1813–1824. doi: 10.1099/mic.0.2008/016923-0 [PubMed: 18524936]

14. Abbott AN, Welsh KJ, Hwang SA, Ploszaj P, Choudhury T, Boyd S, Blackburn MR, Hunter RL Jr., Actor JK. IL-6 mediates 11betaHSD type 2 to effect progression of the mycobacterial cord factor trehalose 6,6'-dimycolate-induced granulomatous response. Neuroimmunomodulation 2011;18:212–225. doi: 10.1159/000323776 [PubMed: 21389736]

15. Donnachie E, Fedotova EP, Hwang SA. Trehalose 6,6-Dimycolate from Mycobacterium tuberculosis Induces Hypercoagulation. The American journal of pathology 2016;186:1221–1233. doi: 10.1016/j.ajpath.2015.12.019 [PubMed: 26968340]

16. Guidry TV, Olsen M, Kil KS, Hunter RL Jr., Geng YJ, Actor JK. Failure of CD1D−/− mice to elicit hypersensitive granulomas to mycobacterial cord factor trehalose 6,6'-dimycolate. Journal of interferon & cytokine research : the official journal of the International Society for Interferon and Cytokine Research 2004;24:362–371. doi: 10.1089/107999004323142222

17. Pelletier M, Forget A, Bourassa D, Gros P, Skamene E. Immunopathology of BCG infection in genetically resistant and susceptible mouse strains. Journal of immunology 1982;129:2179–2185.

18. Collins FM, Congdon CC, Morrison NE. Growth of mycobacterium bovis (BCG) in T lymphocyte-depleted mice. Infection and immunity 1975;11:57–64. [PubMed: 1090526]
19. Hwang SA, Kruzel ML, Actor JK. Oral recombinant human or mouse lactoferrin reduces Mycobacterium tuberculosis TDM induced granulomatous lung pathology. Biochemistry and cell biology = Biochimie et biologie cellulaire 2017;95:148–154. doi: 10.1139/bcb-2016-0061 [PubMed: 28165282]
20. Ryll R, Kumazawa Y, Yano I. Immunological properties of trehalose dimycolate (cord factor) and other mycolic acid-containing glycolipids--a review. Microbiol Immunol 2001;45:801–811. [PubMed: 11838897]
21. Hunter RL, Olsen MR, Jagannath C, Actor JK. Multiple roles of cord factor in the pathogenesis of primary, secondary, and cavitary tuberculosis, including a revised description of the pathology of secondary disease. Annals of clinical and laboratory science 2006;36:371–386. [PubMed: 17127724]
22. Ishikawa E, Mori D, Yamasaki S. Recognition of Mycobacterial Lipids by Immune Receptors. Trends in immunology 2017;38:66–76. doi: 10.1016/j.it.2016.10.009 [PubMed: 27889398]
23. Kato M, Miki K, Matsunaga K, Yamamura Y. Biochemical analysis of the virulence of tubercle bacilli. The American review of respiratory disease 1959;80:535–542. doi: 10.1164/arrd.1959.80.4P1.535 [PubMed: 14404735]
24. Bekierkunst A, Levij IS, Yarkoni E, Vilkas E, Adam A, Lederer E. Granuloma formation induced in mice by chemically defined mycobacterial fractions. J Bacteriol 1969;100:95–102. [PubMed: 4981067]
25. Retzinger GS. Dissemination of beads coated with trehalose 6,6'-dimycolate: a possible role for coagulation in the dissemination process. Experimental and molecular pathology 1987;46:190–198. [PubMed: 3556532]
26. Retzinger GS, Meredith SC, Hunter RL, Takayama K, Kezdy FJ. Identification of the physiologically active state of the mycobacterial glycolipid trehalose 6,6'-dimycolate and the role of fibrinogen in the biologic activities of trehalose 6,6'-dimycolate monolayers. Journal of immunology 1982;129:735–744.
27. Behling CA, Perez RL, Kidd MR, Staton GW Jr., Hunter RL. Induction of pulmonary granulomas, macrophage procoagulant activity, and tumor necrosis factor-alpha by trehalose glycolipids. Annals of clinical and laboratory science 1993;23:256–266. [PubMed: 8373130]
28. Sakamoto K, Geisel RE, Kim MJ, Wyatt BT, Sellers LB, Smiley ST, Cooper AM, Russell DG, Rhoades ER. Fibrinogen regulates the cytotoxicity of mycobacterial trehalose dimycolate but is not required for cell recruitment, cytokine response, or control of mycobacterial infection. Infection and immunity 2010;78:1004–1011. doi: 10.1128/IAI.00451-09 [PubMed: 20028811]
29. Imamura T, Iyama K, Takeya M, Kambara T, Nakamura S. Role of macrophage tissue factor in the development of the delayed hypersensitivity reaction in monkey skin. Cellular immunology 1993;152:614–622. [PubMed: 8258156]
30. Levi M, ten Cate H, van der Poll T. Endothelium: interface between coagulation and inflammation. Critical care medicine 2002;30:S220–224. [PubMed: 12004239]
31. Levi M, van der Poll T. Two-way interactions between inflammation and coagulation. Trends in cardiovascular medicine 2005;15:254–259. doi: 10.1016/j.tcm.2005.07.004 [PubMed: 16226680]
32. Dorhoi A, Kaufmann SH. Perspectives on host adaptation in response to Mycobacterium tuberculosis: modulation of inflammation. Semin Immunol 2014;26:533–542. doi: 10.1016/j.smim.2014.10.002 [PubMed: 25453228]
33. Tsenova L, O'Brien P, Holloway J, Peixoto B, Soteropoulos P, Fallows D, Kaplan G, Subbian S. Etanercept exacerbates inflammation and pathology in a rabbit model of active pulmonary tuberculosis. Journal of interferon & cytokine research : the official journal of the International Society for Interferon and Cytokine Research 2014;34:716–726. doi: 10.1089/jir.2013.0123

- Each article needs to have a financial disclosure line, usually within the author bio section.

Publication of this supplement was supported by The University of Texas Health Science Center at Houston.

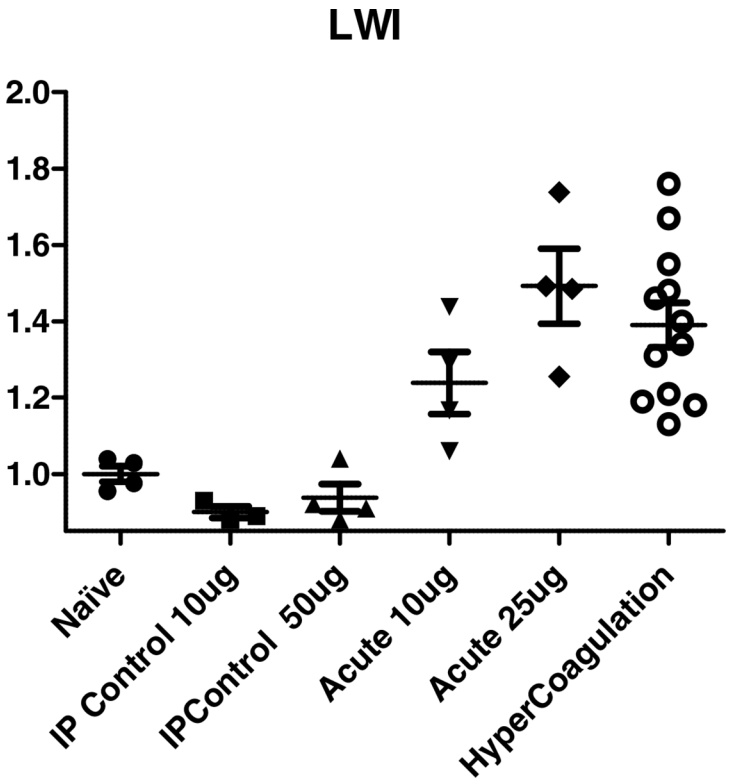

Figure 1. Comparative gross pulmonary reactivity in models of TDM induced pathology.

The lung weight index (LWI) was calculated post TDM administration, as a measure of gross pulmonary inflammation and cellular recruitment. Lungs from mice injected with TDM-IP (10 μg or 50 μg given IP), TDM-IV Acute (10 μg or 25 μg given IV), or TDM-IPIV Hypercoaculation (10 μg IP plus 10 μg IV) were assessed. Lungs were also isolated for comparison to naïve (non-injected) mice. At day 7 post final TDM administration, lungs were collected and weighed, and compared against weight of the mouse. Individual points represent unique animals. Results represent mean ± standard deviation, with similar data obtained from repeated experiments; 4–6 mice per group per experiment.

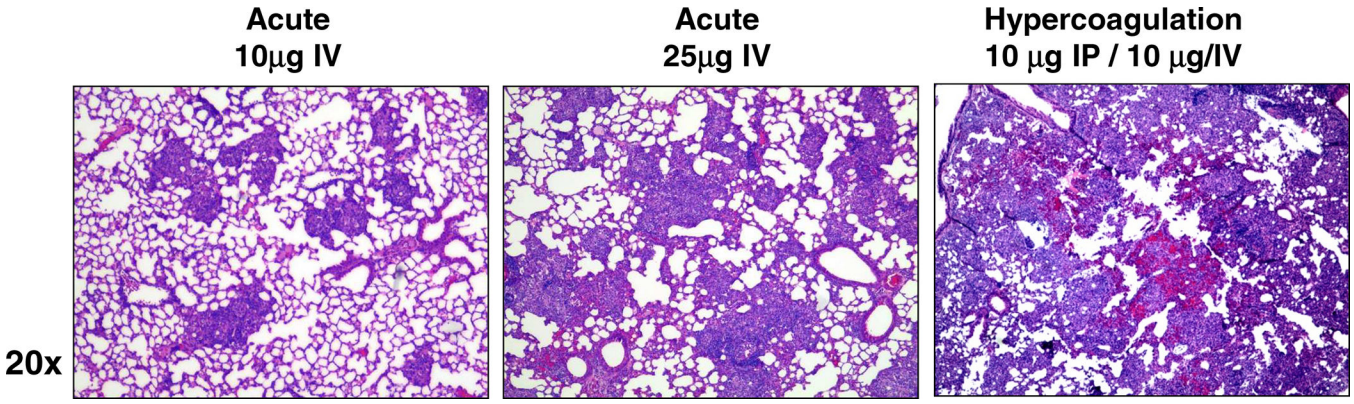

Figure 2. Histological Appearance of Pulmonary Granulomatous Inflammation due to TDM.

TDM was administered as described in the methods, and mice were sacrificed at day 7 post-injection. Histologic examination of lungs revealed acute granulomatous response, increasing with dose of TDM administered, culminating in marked monocytic infiltration and increased cellular aggregation. In contrast, TDM given IP followed 7 days later by IV administration led to marked hemorrhagic response and vascular occlusion. Formalin fixed lung sections were hematoxylin and eosin stained (H&E); representative sections; 20x magnification. Representative sections from repeated experiments; 4–6 mice per group per experiment.

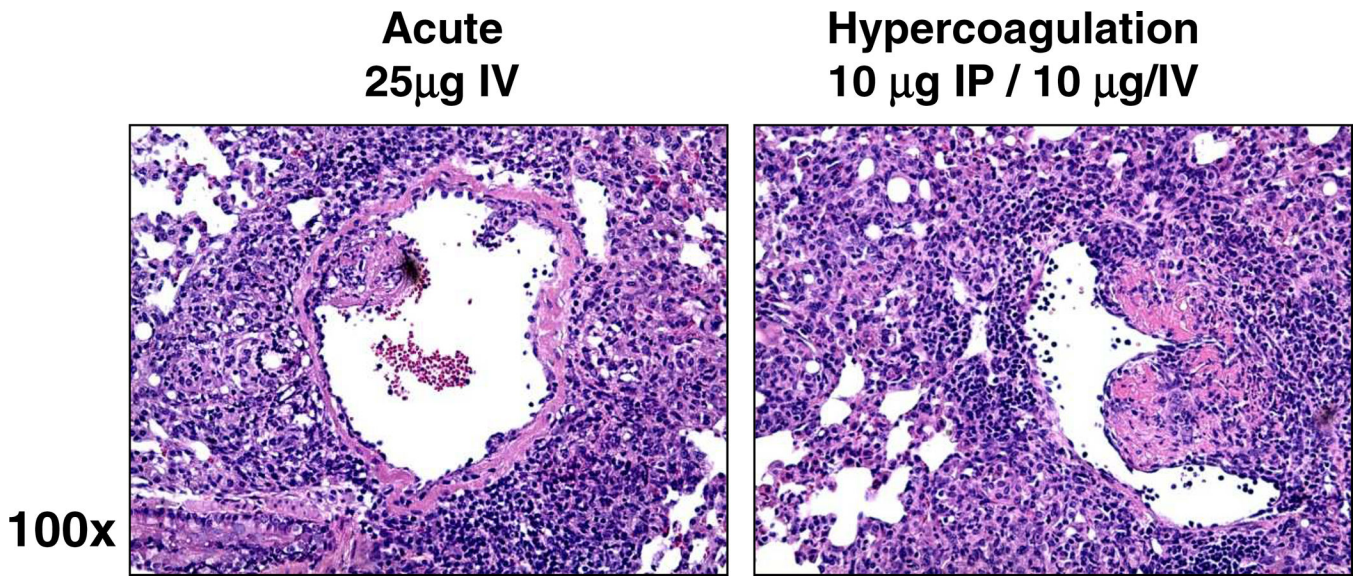

Figure 3. Inflammation Accompanied with Vascular Occlusion in the Hypercoagulation Model Post TDM Administration.

Acute IV administration reveals accumulation of monocytes and lymphocytes surrounding vascular beds, but limited inflammation in subendothelial regions. In contrast, the hypercoagulation model led to aggressive inflammation throughout the parenchmya, with alterations to subendothelial structure lining vasculature. Formalin fixed lung sections; H&E stain; representative sections, 100x magnification. Representative sections from repeated experiments; 4–6 mice per group per experiment.

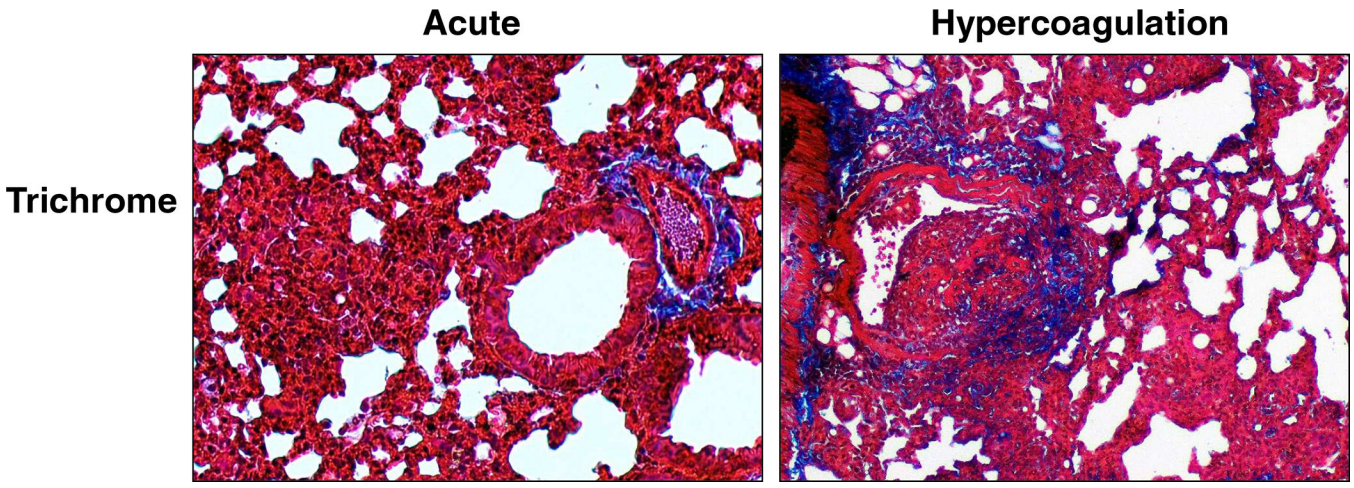

Figure 4. Vascular Remodeling and Collagen Deposition during TDM-Induced Hypercoagulation.

Formalin fixed lung sections were Trichrome stained to assess deposition of collagen material post treatment. Acute inflammation demonstrates no collagen deposition associated with granulomatous response, whereas the hypercoagulation inflammation localized to subendothelial regions shows high matrix formation. Trichrome stain; collagen (blue); representative sections, 100x magnification. Representative sections; 4–6 mice per group per experiment.

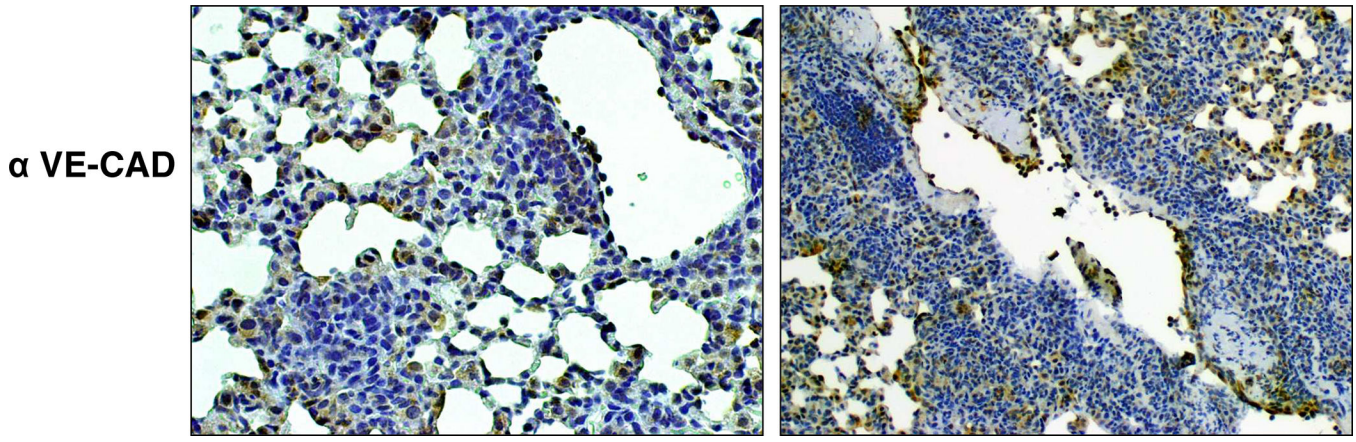

Figure 5. Localization of Inflammation Relative to Vascular Endothelium.

Formalin fixed lung sections were stained with antibody to Vascular Endothelial Cadherin, CD144, (1:200), and visualized using standard HRP techniques. Acute inflammation demonstrates reactivity peripheral to vascular regions, whereas the hypercoagulation inflammation is localized to subendothelial regions, accompanied by relative destruction in continuity of endothelial lined blood vessels. Representative sections, 100x magnification. Representative sections; 4–6 mice per group per experiment.